

Supplementary Materials for

Imaging *Enterobacteriales* infections in patients using pathogen-specific positron emission tomography

Alvaro A. Ordonez, Luz M. Wintaco, Filipa Mota, Andres F. Restrepo, Camilo A. Ruiz-Bedoya, Carlos F. Reyes, Luis G. Uribe, Sudhanshu Abhishek, Franco R. D'Alessio, Daniel P. Holt, Robert F. Dannals, Steven P. Rowe, Victor R. Castillo, Martin G. Pomper, Ulises Granados*, Sanjay K. Jain*

*Corresponding author. Email: ulisesgranados@fcv.org (U.G.); sjain5@jhmi.edu (S.K.J.)

Published 14 April 2021, *Sci. Transl. Med.* **13**, eabe9805 (2021)
DOI: 10.1126/scitranslmed.abe9805

The PDF file includes:

Fig. S1. Mechanism of ^{18}F -FDS accumulation in bacteria.
Fig. S2. Whole-body ^{18}F -FDS PET/CT.
Fig. S3. Biodistribution of ^{18}F -FDS in unaffected tissues.
Fig. S4. Bacterial burden and in vitro ^{18}F -FDS uptake.
Fig. S5. Correlation of ^{18}F -FDS PET with host inflammatory cells.
Fig. S6. ^{18}F -FDS PET target-to-nontarget ratios for all patients.
Fig. S7. Hamster model pathology.
Fig. S8. Patients with false-negative ^{18}F -FDS PET.
Fig. S9. ^{18}F -FDS accumulation in fluids.
Table S1. Selection criteria for patient enrollment in the clinical study.
Table S2. Patient characteristics.
Legend for data file S1
Legends for movies S1 and S2

Other Supplementary Material for this manuscript includes the following:

(available at stm.sciencemag.org/cgi/content/full/13/589/eabe9805/DC1)

Data file S1 (Microsoft Excel format). Individual subject-level data.
Movie S1 (.mp4 format). ^{18}F -FDS PET/CT in a SARS-CoV-2–infected hamster.
Movie S2 (.mp4 format). ^{18}F -FDS PET/CT in a SARS-CoV-2 and *K. pneumoniae* coinfecting hamster.

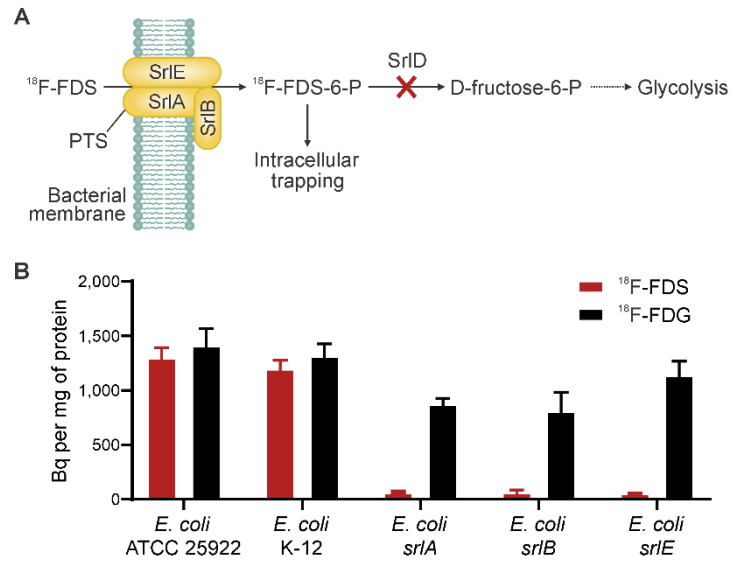


Fig. S1. Mechanism of $^{18}\text{F-FDS}$ accumulation in bacteria. (A) *Enterobacteriales* can utilize sorbitol as a sole carbon source. $^{18}\text{F-FDS}$ uptake in *Enterobacteriales* occurs via a metabolically conserved pathway mediated by a sorbitol-specific phosphoenolpyruvate-dependent, sugar-transporting phosphotransferase system (PTS) (9). In *E. coli*, PTS is composed of three subunits: SrlE, SrlA and SrlB. The *srl* operon is induced by sorbitol, and PTS transports sorbitol with low micromolar affinities (10). Sorbitol 6-phosphate is then oxidized by sorbitol-6-phosphate 2-dehydrogenase (SrlD) into D-fructose 6-phosphate which is subsequently metabolized, primarily via glycolysis. $^{18}\text{F-FDS}$ 6-phosphate is not recognized as a substrate by the highly specific bacterial SrlD and is trapped inside the bacteria. (B) In vitro uptake of $^{18}\text{F-FDS}$ and $^{18}\text{F-FDG}$ at 120 min in *E. coli* ATCC 25922 (reference strain), *E. coli* K-12 (parent strain) and *E. coli* K-12 *srlA*, *srlB*, and *srlE* knockout strains. Data represented as mean and standard deviation ($n = 5$ replicates for each bacterial strain).



Fig. S2. Whole body ^{18}F -FDS PET/CT. Three-dimensional maximum intensity projections 1 h after tracer injection are shown for all 26 patients. The CT is represented in blue, while the ^{18}F -FDS PET signal is represented in orange-red. All images are represented using the same standardized uptake value (SUV) scale (0-5).

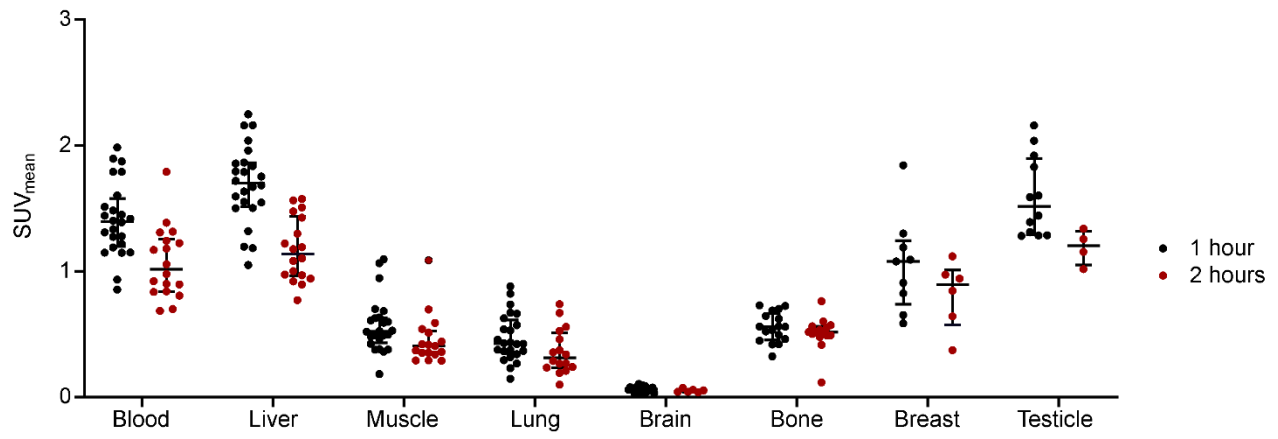


Fig. S3. Biodistribution of ^{18}F -FDS in unaffected tissues. The mean standardized uptake value (SUV_{mean}) derived from ^{18}F -FDS PET for all 26 patients at 1 h (black) and 2 h (red) after tracer injection is shown. Data is represented as median and IQR.

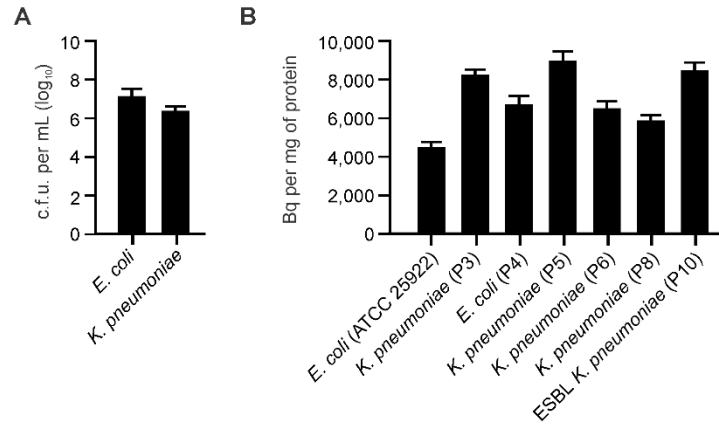


Fig. S4. Bacterial burden and in vitro ¹⁸F-FDS uptake. (A) Bacterial burden in biological samples collected from patients with *E. coli* or *K. pneumoniae* infections. Data represented as mean and standard deviation (n = 3 isolates for each strain). (B) In vitro ¹⁸F-FDS uptake in *Enterobacteriales* strains (including one MDR, ESBL-producing strain) isolated from infected patients from this study compared to a reference strain (*E. coli* ATCC 25922). Data represented as mean and standard deviation (n = 6 replicates for each strain).

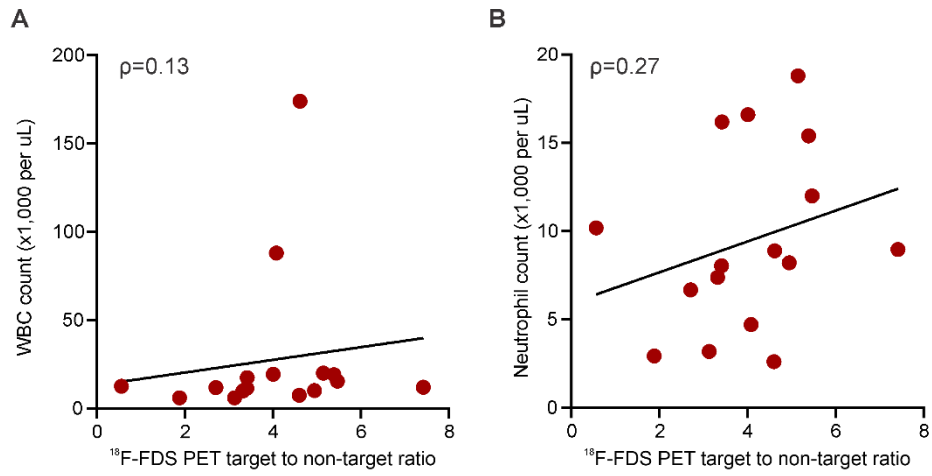


Fig. S5. Correlation of ^{18}F -FDS PET with host inflammatory cells. Correlation of ^{18}F -FDS PET target to non-target ratio 2 h post-injection with (A) peripheral white blood cell (WBC) counts (Pearson $\rho = 0.13$, $P = 0.62$) and (B) peripheral neutrophil counts (Pearson $\rho = 0.27$, $P = 0.30$).

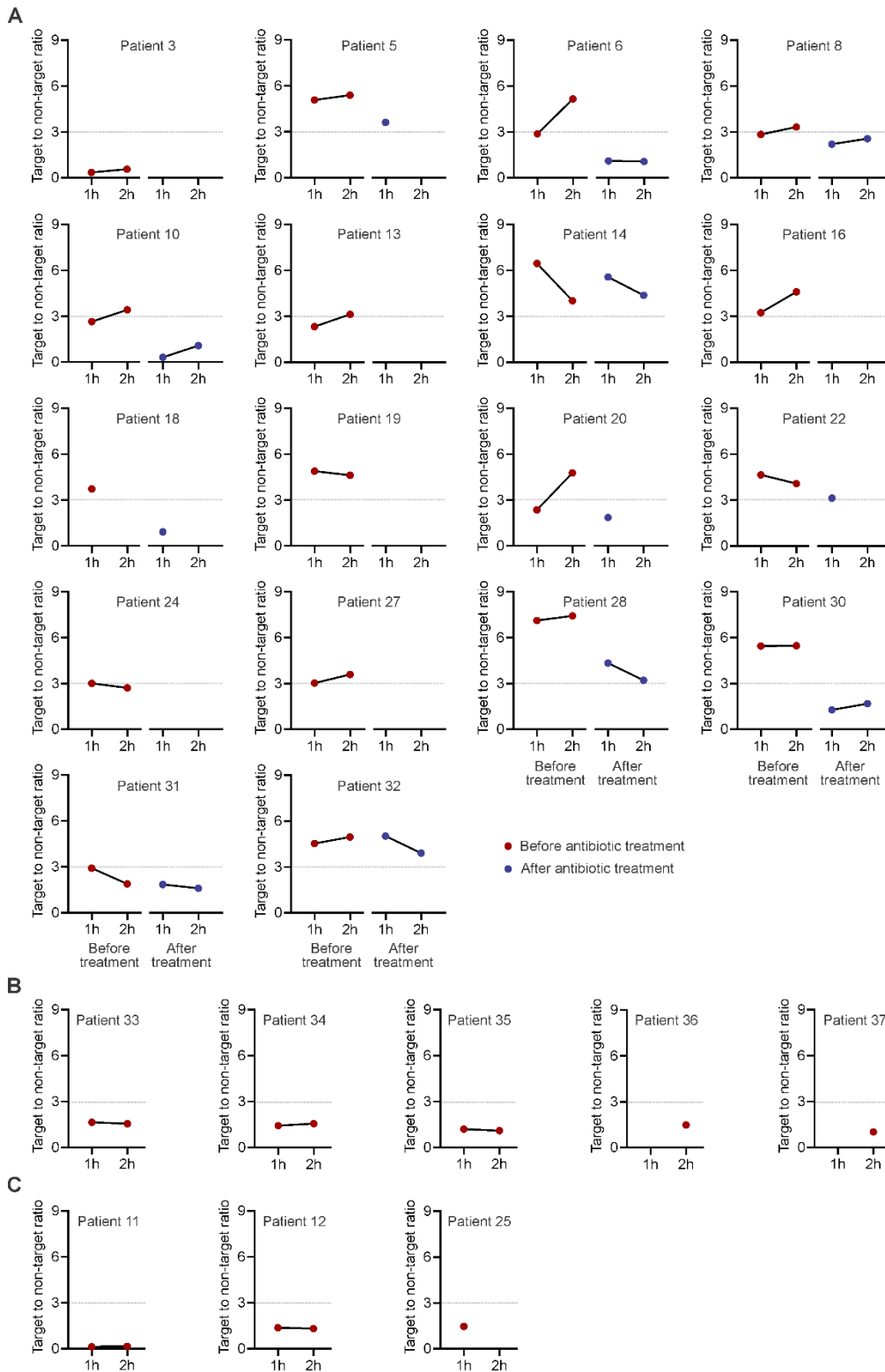


Fig. S6. ^{18}F -FDS PET target-to-nontarget ratios for all patients. ^{18}F -FDS PET target-to-non-target ratio at 1 and 2 h after tracer injection are shown for all 26 patients. **(A)** Microbiologically confirmed *Enterobacterales* infection, and the subset of patients imaged again after completion of antibiotic treatment. **(B)** Confirmed inflammatory or oncological disease and **(C)** microbiologically confirmed infections due to non-*Enterobacterales*. The dotted line indicates the target-to-nontarget ratio cut off of 3, determined in this study to be indicative of infection.

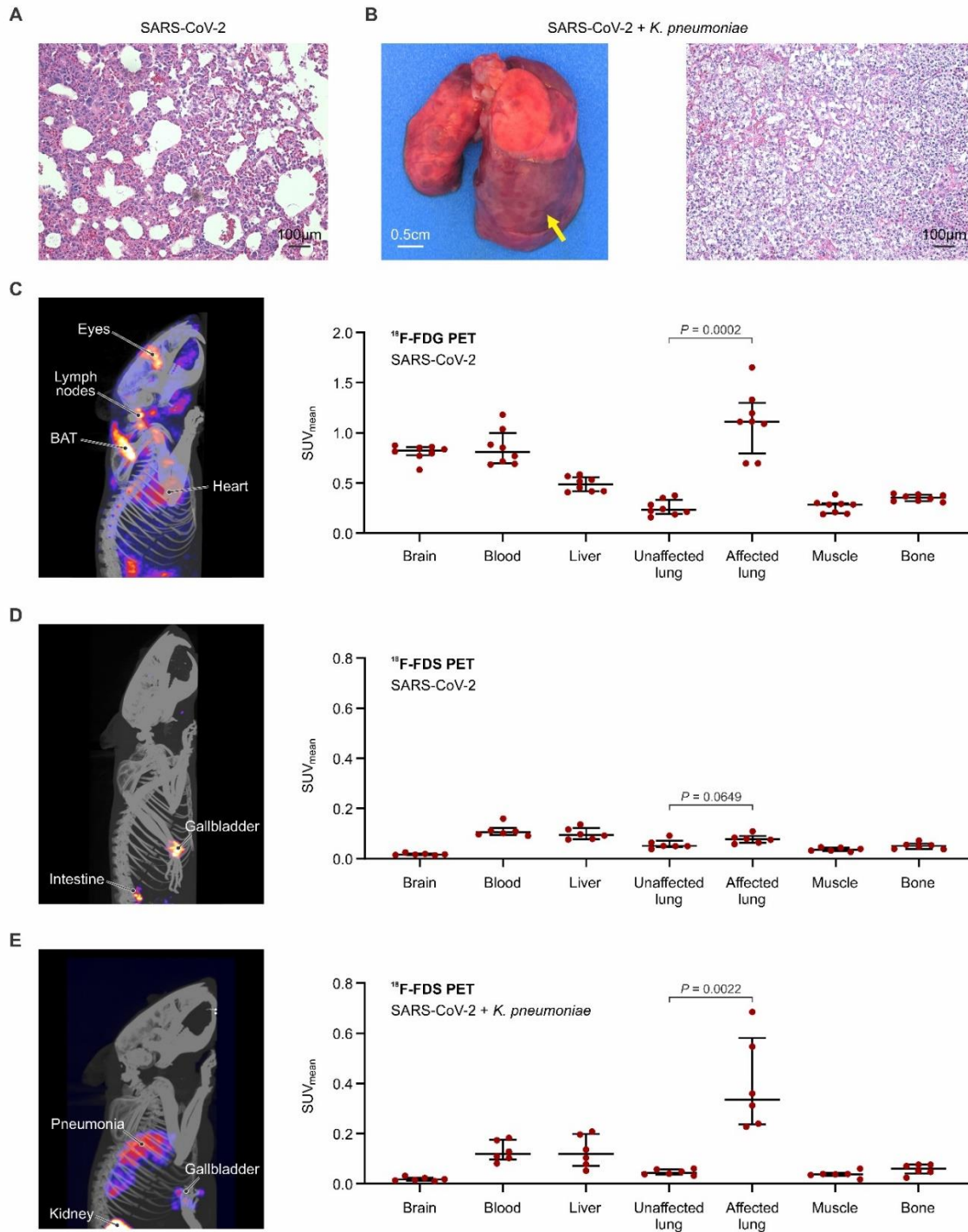


Fig. S7. Hamster model pathology. (A) Hematoxylin and eosin (H&E) staining of lungs from a representative SARS-CoV-2-infected hamster 7 days post-infection. (B) Gross pathology (yellow arrow indicates affected area) and histology (H&E) of the lungs of a hamster infected with SARS-CoV-2 and *K. pneumoniae*. (C) Three-dimensional maximum intensity projection (MIP) of an animal infected with SARS-CoV-2 and imaged with ¹⁸F-FDG and corresponding tissue biodistribution for all animals (n = 8) represented as mean standardized uptake value (SUV_{mean}). (D) ¹⁸F-FDS PET/CT MIP of an animal infected with SARS-CoV-2 and corresponding tissue biodistribution for all animals (n = 6). (E) ¹⁸F-FDS PET/CT MIP of an animal infected with SARS-CoV-2 and *K. pneumoniae* and corresponding tissue biodistribution for all animals (n = 6). Data is represented as median and IQR. Statistical comparisons performed using a two-tailed Mann-Whitney *U* test. BAT, brown adipose tissue.

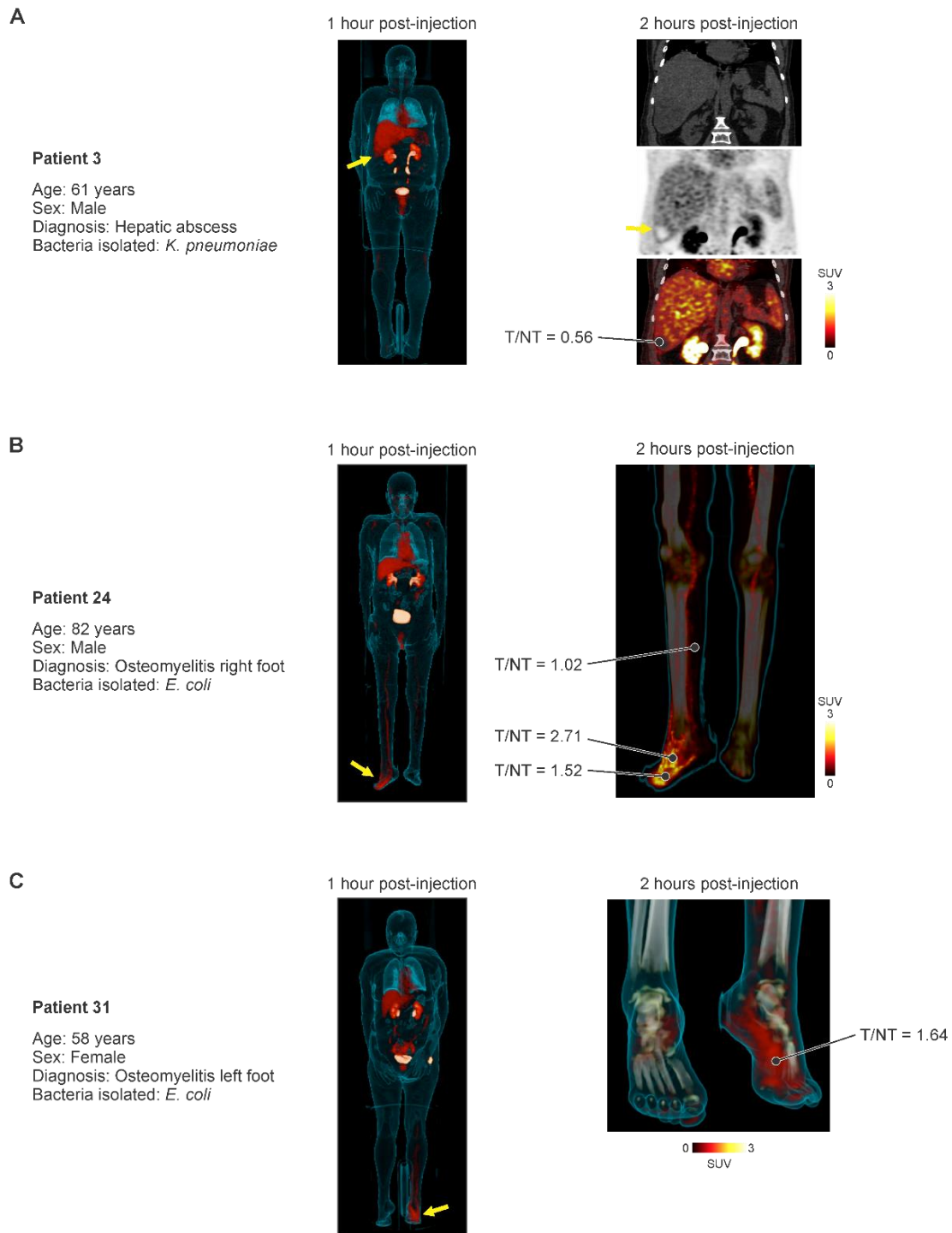


Fig. S8. Patients with false-negative ^{18}F -FDS PET. (A) Three-dimensional maximum intensity projection (MIP) shown on the left, coronal CT (top), PET (middle), and overlaid PET/CT (bottom) shown on the right from 61-year-old male presenting with a hepatic abscess due to *K. pneumoniae* with a focus of photopenia (arrow). (B and C) Three-dimensional MIP for whole body (left panels) and localized site of infection (right panels) from two patients with diabetes with microbiologically confirmed foot osteomyelitis. While a higher ^{18}F -FDS signal can be visually assessed at the infection site, the target-to-nontarget tissue ratio (TNT) is below the cutoff of 3. The yellow arrows point to the site of infection.

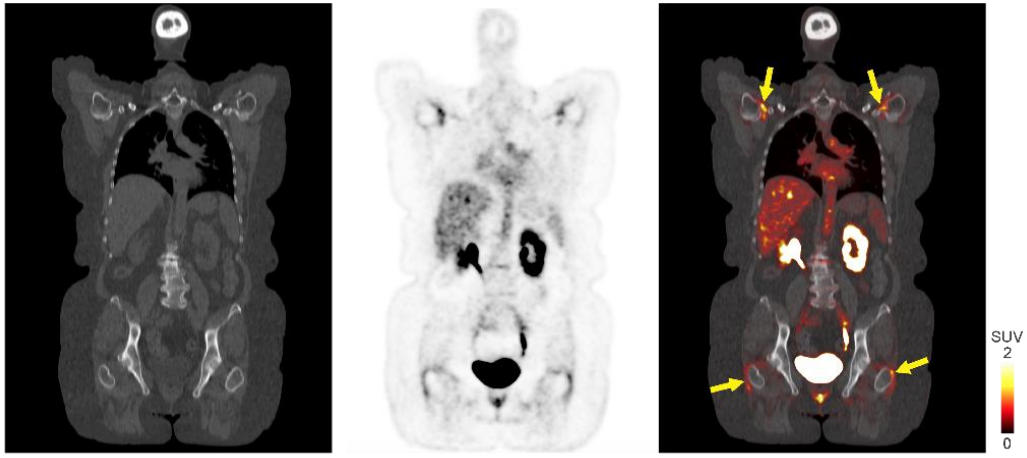


Fig. S9. ¹⁸F-FDS accumulation in fluids. Coronal CT (left), PET (middle), and overlaid PET/CT (right) from a patient with interstitial lung disease. ¹⁸F-FDS PET signal was observed in the synovial fluid (yellow arrows).

Table S1. Selection criteria for patient enrollment in the clinical study.

- Greater than or equal to 18 years old
- Patients with microbiologically confirmed *Enterobacterales* infection OR with high suspicion for *Enterobacterales* infection with microbiological-confirmation anticipated within 72 hours of imaging:
 - Received no or \leq 72 hours of antibiotic treatment for the current episode of infection by the time of first ^{18}F -FDS PET/CT
 - Microbiological-confirmation was defined as the isolation of bacteria from a sample obtained directly from the infection site
 - Patients with suspected infection without microbiological-confirmation were excluded from the study analysis
- Control patients: Confirmed inflammatory or oncologic disease and clinically determined not to have an infection
- Determined by the patient's medical team to be stable to participate in the study
- Not pregnant
- Serum creatinine $<$ 3 times the upper limit of normal
- Total bilirubin $<$ 3 times the upper limit of normal
- Liver transaminases $<$ 5 times the upper limit of normal
- Not treated with an investigational drug, biologic, or therapeutic device within 30 days prior to the ^{18}F -FDS PET/CT
- Adequate venous access
- Ability to provide written informed consent

Table S2. Patient characteristics.

ID	Age (years)	Sex	Weight (kg)	Diagnosis	Comorbidities	Pathogen isolated	Sample obtained from	Neutrophil count (x10 ³ /μL)	Notes
1	54	F	53	Brain abscess	Chagas disease	No sample	-	7.20	Excluded
2	69	M	74	Pneumonia	DM	<i>Raoultella planticola</i>	BAL	6.07	Excluded
3	61	M	84	Hepatic abscess	DM, CKD	<i>Klebsiella pneumoniae</i>	Abscess drainage	10.20	
4	44	F	60	Peritonitis	Abdominal trauma	<i>Escherichia coli</i> and <i>Klebsiella pneumoniae</i>	Peritoneal fluid	5.81	Excluded
5	67	M	59	Pneumonia	Lung cancer	<i>Klebsiella pneumoniae</i>	BAL	15.40	
6	35	F	69	Abdominal abscess	Gastric cancer	<i>Klebsiella pneumoniae</i>	Abscess drainage	18.80	
7	33	M	55	Abdominal collection	Appendicitis, post-surgery	Negative cultures	Collection drainage	8.64	Excluded
8	70	M	70	Pleural empyema	-	<i>Klebsiella pneumoniae</i>	BAL	7.39	
9	63	F	73	Hepatic abscess	DM, CKD	<i>Escherichia coli</i>	Abscess drainage	12.40	Excluded
10	38	M	69	Intracranial infection	Urachal cancer	ESBL <i>K. pneumoniae</i>	CSF and wound drainage	16.20	
11	31	M	65	Hepatic abscess	-	<i>Entamoeba histolytica</i>	Abscess drainage	11.90	
12	35	F	35	Bronchitis / pneumonia	Asthma	<i>Pseudomonas aeruginosa</i>	BAL	3.88	
13	60	F	42	Bronchiectasis exacerbation	-	<i>Klebsiella pneumoniae</i>	BAL	3.19	
14	33	M	63	Infected bone fracture	Leg trauma	ESBL <i>E. coli</i>	Tissue sample	16.60	
15	70	M	73	Fournier gangrene	DM	<i>Klebsiella pneumoniae</i>	Tissue sample	15.40	Excluded
16	65	F	92	Cellulitis right arm	Breast cancer	<i>Klebsiella aerogenes</i>	Tissue sample	2.62	
17	70	M	57	Sacral ulcer	DM	<i>Escherichia coli</i>	Tissue sample	17.40	Excluded
18	69	M	65	Pneumonia	COPD	<i>Klebsiella pneumoniae</i>	BAL	15.20	
19	64	M	80	Pneumonia and aspergillosis	AML	<i>Enterobacter cloacae</i>	BAL	8.89	
20	78	M	60	Pneumonia	Gastric cancer	<i>Klebsiella pneumoniae</i>	BAL	9.36	

21	74	M	84	Abdominal collection	Nephrectomy	<i>Citrobacter freundii</i> and <i>Klebsiella pneumoniae</i>	Collection drainage	7.81	Excluded
22	59	M	83	Ischiorectal abscess	Fournier gangrene	ESBL <i>E. coli</i>	Tissue sample	4.72	
23	68	M	83	Pneumonia	Lung cancer	Negative cultures	Lung biopsy	11.20	Excluded
24	82	M	68	Osteomyelitis right foot	DM, PAD	<i>Escherichia coli</i>	Tissue sample	6.68	
25	74	F	52	Pneumonia	Osteoporosis	<i>Mycobacterium tuberculosis</i>	BAL	3.81	
26	53	M	45	Abdominal collection	Pancreatitis, post-ERCP	<i>Klebsiella aerogenes</i>	Blood	4.01	Excluded
27	51	F	60	Pneumonia	Pulmonary embolism	<i>Klebsiella pneumoniae</i>	BAL	8.05	
28	91	M	91	Pneumonia	COPD, prostate cancer	ESBL <i>K. pneumoniae</i>	BAL	8.97	
29	78	M	70	Subscapular abscess	Hypertension	Gram negative bacilli from stain	Abscess drainage	6.19	Excluded
30	41	F	101	Cellulitis left arm	Obesity, hypertension	<i>Serratia marcescens</i>	Tissue sample	12.00	
31	58	F	60	Osteomyelitis left foot	DM, PAD	<i>Escherichia coli</i>	Tissue sample	2.94	
32	67	F	59	Cellulitis left breast	Breast cancer, DM	<i>Klebsiella aerogenes</i>	Tissue sample	8.22	
Patients with inflammatory and/or oncological disease without infection									
33	64	M	93	Interstitial lung disease	-	-	-	-	
34	60	M	74	Interstitial lung disease	-	-	-	-	
35	59	F	84	Interstitial lung disease	-	-	-	-	
36	54	M	86	Interstitial lung disease	-	-	-	-	
37	64	M	89	Breast cancer	-	-	-	-	

Table notes: Type 2 diabetes mellitus (DM), chronic kidney disease (CKD), acute myeloid leukemia (AML), peripheral artery disease (PAD), endoscopic retrograde cholangiopancreatography (ERCP), bronchoalveolar lavage (BAL), extended-spectrum betalactamase (ESBL), cerebrospinal fluid (CSF), chronic obstructive pulmonary disease (COPD).

Data file S1. Individual subject-level data. (Excel file)

Movie S1. ^{18}F -FDS PET/CT in a SARS-CoV-2-infected hamster. CT (left) and PET/CT overlay (right) of ^{18}F -FDS in a representative animal infected with SARS-CoV-2. ^{18}F -FDS signal is observed in the kidneys, gallbladder and intestine due to normal excretion.

Movie S2. ^{18}F -FDS PET/CT in a SARS-CoV-2 and *K. pneumoniae* coinfecting hamster. CT (left) and PET/CT overlay (right) of ^{18}F -FDS in a representative animal infected with SARS-CoV-2 and *K. pneumoniae*.